

Dynamics of Attached Cavities on Bodies of Revolution

S. L. Ceccio¹

C. E. Brennen

California Institute of Technology,
Pasadena, CA 91125

Attached cavitation was generated on two axisymmetric bodies, a Schiebe body and a modified ellipsoidal body (the I. T. T. C. body), both with a 50.8 mm diameter. Tests were conducted for a range of cavitation numbers and for Reynolds numbers in the range of $Re = 4.4 \times 10^5$ to 4.8×10^5 . Partially stable cavities were observed. The steady and dynamic volume fluctuations of the cavities were recorded through measurements of the local fluid impedance near the cavitating surface using a series of flush mounted electrodes. These data were combined with photographic observations. On the Schiebe body, the cavitation was observed to form a series of incipient spot cavities which developed into a single cavity as the cavitation number was lowered. The incipient cavities were observed to fluctuate at distinct frequencies. Cavities on the I. T. T. C. started as a single patch on the upper surface of the body which grew to envelope the entire circumference of the body as the cavitation number was lowered. These cavities also fluctuated at distinct frequencies associated with oscillations of the cavity closure region. The cavities fluctuated with Strouhal numbers (based on the mean cavity thickness) in the range of $St = 0.002$ to 0.02 , which are approximately one tenth the value of Strouhal numbers associated with Kármán vortex shedding. The fluctuation of these stabilized partial cavities may be related to periodic break off and filling in the cavity closure region and to periodic entrainment of the cavity vapor. Cavities on both headforms exhibited surface striations in the streamwise direction near the point of cavity formation, and a frothy mixture of vapor and liquid was detected under the turbulent cavity surface. As the cavities became fully developed, the signal generated by the frothy mixture increased in magnitude with frequencies in the range of 0 to 50 Hz.

1 Introduction

“Fixed” or “attached” cavitation occurs when a liquid flow detaches from the rigid boundary of an immersed body or flow passage to form a cavity, and this cavity may exist indefinitely with a quasi-steady geometry. Attached cavitation may negatively affect the performance of hydromechanic surfaces, as in the case of propeller thrust breakdown (Emerson and Sinclair 1967). It is associated with cavitation erosion damage in hydraulic turbomachinery and marine propellers (Knapp et al., 1970), and is responsible for dangerous ship propeller/hull interactions (Weitendorf, 1989) and unwanted acoustic emissions (Blake et al., 1977). All of these phenomena are influenced by cavity dynamics, but studies of cavity fluctuations have been hampered by the lack of simple, nonintrusive cavity volume measurement techniques.

Previous researchers have used high speed films (Knapp, 1955 and Lush and Skipp, 1986) and near cavity LDA measurements (Avellan et al., 1988) to observe cavity dynamics. Presented here are the initial results of a different method to study the time averaged and unsteady nature of attached cavities using electrical impedance measurements of the near-surface fluid with flush mounted electrodes. This technique has

recently been used to study travelling bubble cavitation (Ceccio and Brennen, 1991), and the same experimental setup and techniques were employed by this study.

2 Experimental Methods

Attached cavities were produced on three axisymmetric headforms made of lucite: one Schiebe body and two modified ellipsoid bodies (known as I. T. T. C. headforms), which are described below. The experiments were conducted in the Low Turbulence Water Tunnel (LTWT) at the California Institute of Technology. (Gates 1977). The free-stream velocity, U , for these tests was varied from 8.3 to 9.5 m/s, and for all tests, the velocity of the tunnel was maintained constant. The test section pressure, P , was slowly reduced until the desired operating point was reached. The controlled air content of the water was 6–7 ppm for these tests.

The Schiebe headform used in the experiment had a maximum diameter of 51.4 mm and a minimum pressure coefficient, C_p , of -0.75 (Gates et al., 1979). The actual final diameter of the body, D , is 50.8 mm due to some truncation of the after body. The body was constructed of lucite and was instrumented with three surface electrodes made of silver epoxy. The electrodes were circumferential rings and located at positions $s/D = 0.608$, 0.645 , and 0.691 , where s is the streamwise coordinate measured along the body surface from the stagnation point. The electrodes had a thickness of 0.76 mm. Both

¹Currently at the Department of Mechanical Engineering and Applied Mechanics, University of Michigan, Ann Arbor, Mich.

Contributed by the Fluids Engineering Division for publication in the JOURNAL OF FLUIDS ENGINEERING. Manuscript received by the Fluids Engineering Division April 13, 1991.

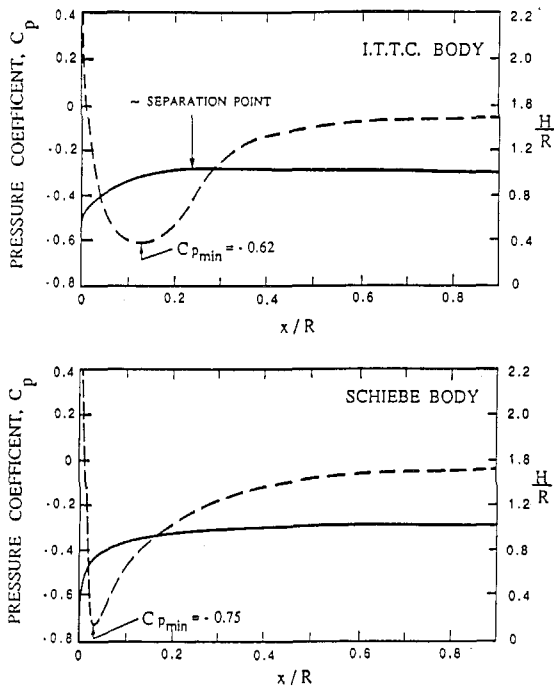


Fig. 1 Profile and surface pressure distribution on the Schiebe and I. T. T. C. bodies

I. T. T. C. bodies (Lingren and Johnsson, 1966) were of identical shape but were instrumented with different electrode geometries. The minimum pressure coefficient for the I. T. T. C. body is -0.62 , and the diameter of the bodies was 50.4 mm. The first I. T. T. C. body was instrumented with sixteen circumferential electrodes of thickness 0.76 mm and equally spaced 2.54 mm apart in the longitudinal direction starting at $s/D = 0.68$ and ending at $s/D = 1.37$. The second I. T. T. C. headform had rectangular patch electrodes of width 1.14 mm in the streamwise direction and length 5.72 mm in the circumferential direction. They were equally spaced 2.54 mm apart in the longitudinal direction starting at $s/D = 0.68$ and ending at $s/D = 1.37$. The surface of the bodies, including the electrode-lucite interface, was highly polished, and no surface cavitation was observed to consistently form on the electrode/lucite interface which would have implied significant local roughness. The headform profiles and surface pressure distributions are presented in Fig. 1.

The electrodes were used to measure both the mean volume and volume fluctuations of the attached cavities. An alternating potential of fixed amplitude is applied to each electrode, and neighboring electrodes have voltage signals which are 180 degrees out of phase. Changes in the emitted current are measured for each electrode. When a void or cavity is present over

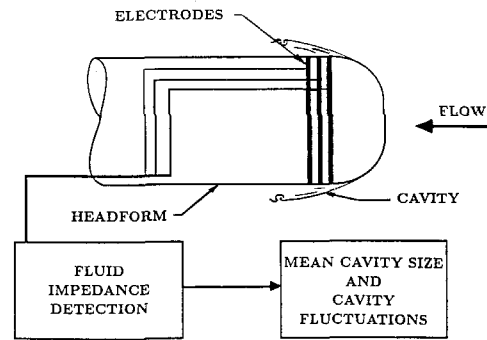


Fig. 2 Schematic diagram of fluid impedance measuring system

a portion of the electrode, the fluid impedance is increased, decreasing the emitted current. In the case of attached cavitation, changes in the electrode signal are the result of two separate effects. First, the percentage of the electrode surface area which will freely conduct electricity is reduced, and hence the magnitude of the output current decreases. This is the primary effect detected by the electrode system. There may also be a secondary effect due to changes in conductivity of the cavity content, which consists of a liquid and vapor mixture; the conductivity of this mixture will clearly differ from that of water.

The dynamic response of the electrode signal processor is on the order of 10 kHz, and the signal to electrical noise ratio was at least 45 dB for all the experiments. A complete description of the electrode system is provided by Ceccio (1990). The Fourier transforms of the electrode signal were performed digitally with a windowed FFT algorithm, and the error estimates which accompany the FFTs were derived from baseline measurements. In addition to the electrical measurements, high speed still photographs of the attached cavities were taken for each operating condition. From these photographs, the mean cavity thickness and length could be measured, and the cavitation present over each electrode could be recorded. A schematic diagram of the electrode system is shown in Fig. 2.

3 Experimental Results-Schiebe Body Measurements

Originally the Schiebe body shape was designed to avoid the occurrence of laminar separation (Schiebe, 1972) which has been associated with the presence of attached cavities (Arakeri and Acosta, 1973). The experiments were conducted in a fairly narrow range of Reynolds number ($Re = 4.4 \times 10^5 - 4.8 \times 10^5$, based on the body diameter, D). The cavitation formation index, defined as the first appearance of attached cavitation anywhere on the headform, was about $\sigma_{ia} = 0.40$ for all experiments. The leading edge cavitation was located at about $s/D = 0.45$. The cavitation disappearance index, which was always greater than the formation index, was about $\sigma_{da} = 0.42$.

Nomenclature

C_p = pressure coefficient $(P_s - P)/(1/2\rho U^2)$	P_v = water vapor pressure	δ_c = mean cavity thickness
D = diameter of the axisymmetric body	R = radius of headform	ν = kinematic viscosity of water
E = electrode signal voltage	Re = Reynolds number (UD/ν)	ρ = density of water
f = frequency	s = streamwise coordinate measured along the body surface from the stagnation point	σ = cavitation number $(P - P_v)/(1/2\rho U^2)$
H = local radius of headform	St = Strouhal number $(f\delta_c/U)$	σ_{ia} = attached cavitation formation index
L = mean cavity length	U = freestream velocity	σ_{da} = attached cavitation desinence index
P = freestream pressure	x = coordinate along centerline of body	
P_s = pressure on surface of body		

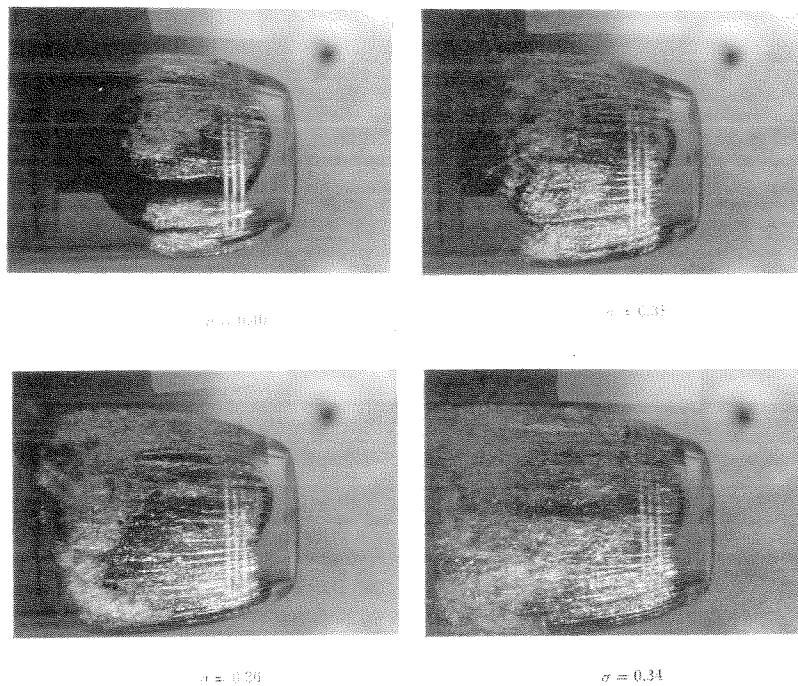


Fig. 3 Examples of attached cavities on the Schiebe body for cavitation numbers $\sigma = 0.40, 0.38, 0.36,$ and 0.34 at a free-stream velocity $U = 9$ m/s

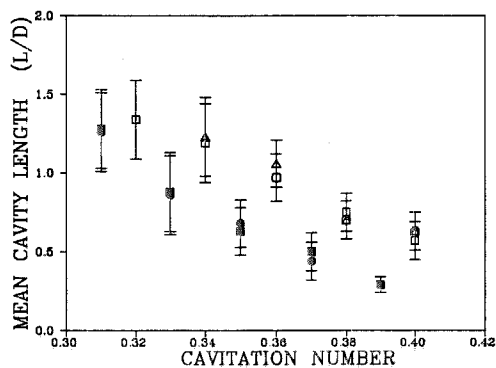


Fig. 4 Mean cavity length plotted against the cavitation number, σ , for the Schiebe body (open symbols) and the I. T. C. body (filled symbols). $U = 8.75$ m/s (\circ), $U = 9$ m/s (Δ), and $U = 9.5$ m/s (\square). The error bars represent the minimum and maximum cavity length measured from the photographs. The value for the I. T. C. body at $\sigma = 0.39$ is the maximum length of the partial cavity.

Photographs taken at each operating point were used as a reference for the electrode data, and examples are presented for the Schiebe body in Fig. 3, with $U = 9$ m/s and $\sigma = 0.40, 0.38, 0.36, 0.34$. At the first formation of cavities, the circumference of the headform was only about half covered with attached patch cavities, or "finger" cavities, some of which were temporally intermittent. At lower cavitation numbers these finger cavities combined to cover the entire circumference of the body. Further decreases in cavitation number increased the mean length of the cavity, L , which is plotted against cavitation number in Fig. 4. The surface of the cavity shows a transition from a smooth laminar interface to a wavy and then turbulent surface in a manner similar to the growth of Tollmein-Schlichting waves in an unstable boundary layer (Brennen, 1970). The point of transition on the cavity surface was about one half the total cavity length in all cases.

Both the mean and fluctuating components of the electrode output contain interesting information. First, the mean level of the electrode signal, E , indicates the percentage of the elec-

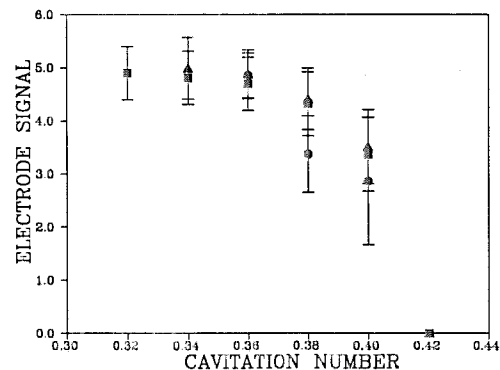


Fig. 5 Mean and standard deviation of the electrode signal, E , from cavitation on the Schiebe body plotted against cavitation number, σ . Vertical scale is arbitrary. $U = 8.75$ m/s (\circ), $U = 9$ m/s (Δ), and $U = 9.5$ m/s (\square).

trode which is covered by the cavity, and this is presented as a function of the cavitation number in Fig. 5. As the cavitation number decreases, the percentage of the circumference covered by the cavity grows, and hence the electrode signal voltage increases. The signal levels off as the cavity become fully developed. The large uncertainty associated with the measurements at higher cavitation numbers is due to the temporal intermittency of the cavitation. Once the cavity is fully developed, the uncertainty decreases. The high frequency portion of the signal is associated with churning of the two-phase mixture inside the cavity and fluctuations of the cavity boundary. The relative contribution of these effects to the signal is small when compared to the portion of the signal resulting from the presence or absence of the cavity. Consequently, the ordinate in Fig. 5 may be transposed into a quantitative measurement of the covered surface when the mean signal is considered.

Secondly, the fluctuating components of the electrode signals were analyzed. Initial spectra obtained without filtering indicated that there were no frequencies of significant magnitude above 500 Hz. Therefore, the fluctuating signal was

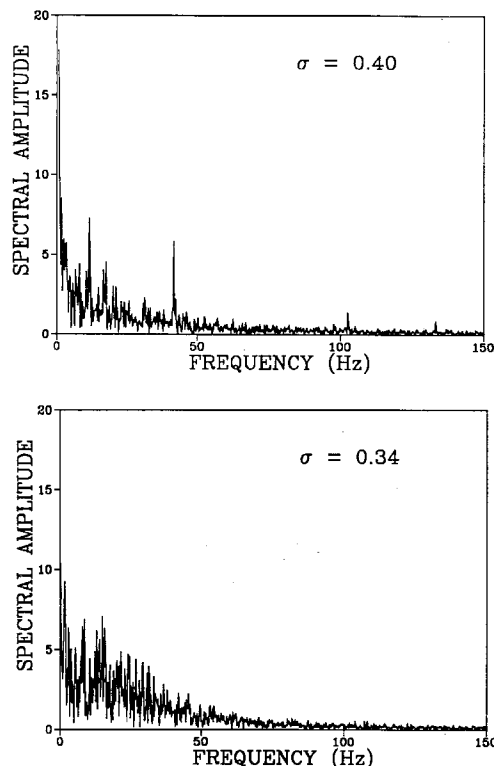


Fig. 6 Electrode signal spectra for cavitation on the Schiebe body. Cavitation number $\sigma = 0.40$ and 0.34 at free-stream velocity $U = 9$ m/s. Vertical scale is arbitrary and the uncertainty of the spectral coefficients is ± 0.20 .

low pass filtered with a cutoff frequency of 1 kHz and was digitally sampled at 2 kHz. This filtering eliminated the signals produced by travelling bubbles which may pass over portions of the uncovered electrodes. Figure 6 represents two typical spectra. They have similar shapes with large amplitudes at low frequency and a uniform rolloff to approximately 500 Hz.

At the higher cavitation numbers, the frequencies below 1 Hz are dominant, since the temporal intermittency associated with the partially developed cavities produces this low frequency component. A series of dominant spectral peaks at intermediate frequencies were detected for the partially developed cavities. As seen in Fig. 6, the spectra for $\sigma = 0.40$ and $U = 9$ m/s has distinct frequency peaks at $f = 10, 40, 103,$ and 133 Hz. These peaks are not due to line noise, are repeatable, and disappear after the cavities became fully developed. Since they occur only when the cavities are partially developed, they may be due to pulsation of the finger cavities in the circumferential direction (see Fig. 7). Note that the electrode location is upstream of the cavity collapse region, which also fluctuates. The Strouhal number, St , based on the cavity mean thickness, δ_c , and upstream velocity, U , for the observed dominant frequencies would be $St = 0.002, 0.006, 0.015,$ and 0.019 , respectively. The cavity thicknesses were derived from the photographs. The error associated with the Strouhal number measurement is approximately ± 20 percent for the cavities with $\sigma > 0.37$ (thin cavities) and ± 25 percent for the cavities with $\sigma < 0.37$ (thick cavities).

As the cavities become fully developed, the magnitudes of frequency component below 1 Hz decrease with increases at higher frequencies, as seen in Fig. 6 for the case of $\sigma = 0.34$. The electrodes on the Schiebe body were located under a portion of the finger cavities which contained only vapor (that is, before complete transition to a turbulent cavity interface). Given the absence of a frothy mixture over the electrodes, two other mechanisms can be cited for the perturbation of the electrode signal. First, the fully developed cavity consists of a

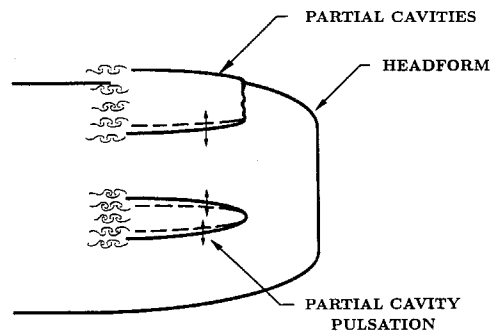


Fig. 7 One possible mode of cavity oscillation

collection of finger cavities whose boundaries may wet the electrode surface. As these boundaries fluctuate, a signal is generated. Secondly, the cavity surface may intermittently collapse, wetting the surface and producing a signal. Fluctuations on the cavity surface due to the presence of Tollmein-Schlichting waves have been estimated to occur with frequencies in the range of 5–10 kHz (Brennen, 1970); signals in this frequency range were not observed. The spectra due to the fully developed cavities revealed no dominant frequencies.

4 Experimental Results-I. T. T. C. Body Measurements

The I. T. T. C. body is known to possess a region of laminar separation which is associated with the formation of stable attached cavities (Arakeri and Acosta, 1973). These cavities originate within the laminar separation bubble. A single cavity first formed at the upper portion of the headform in the region of laminar separation and grew to envelope the entire circumference of the headform as the cavitation number was lowered. This "top to bottom" cavity formation was caused by the slight pressure difference across the headform resulting from gravity, an effect which was not as noticeable on the Schiebe body due to the finger cavity intermittency. The experiments were conducted over a narrow range Reynolds numbers ($Re = 4.4 \times 10^5 - 4.8 \times 10^5$) which resulted in a fairly constant cavity formation index of $\sigma_{ia} = 0.41$. The cavitation disappearance index was $\sigma_{da} = 0.42$. The leading edge of the cavity first appears at approximately $s/D = 0.75$, and the location of the leading edge moved forward as the cavitation number decreased.

The mean cavity length in the streamwise direction presented as a function of cavitation number in Fig. 4. The ratio of cavity length to body diameter (L/D) for the I. T. T. C. headform is consistently lower than that for the Schiebe body at higher cavitation numbers. This is due to the process of cavity formation. In the case of the Schiebe body, the cavities are not promoted by the presence of a laminar separation region and take the form of long cavities close to the headform surface. Cavities on the I. T. T. C. headform first form in the separated recirculating region and are initially confined there at higher cavitation numbers. As the cavitation number decreases, the cavities grow and begin to dominate the flow near headform surface. At this point, the detailed shape of the headform has less influence on the cavity size, hence the ratio (L/D) begins to converge for both axisymmetric bodies.

As in the case of the Schiebe body, the cavity near the separation point consisted of a series of finger cavities or surface striations which, at lower cavitation numbers, combined to cover the circumference of the body. Figure 8 presents photographs of cavitation on this body for the case of free-stream velocity $U = 8.7$ m/s and for cavitation numbers of $\sigma = 0.37, 0.35, 0.33, 0.31$. The finger cavities were less well defined than those of the Schiebe body. This may be due to the relatively short distance from the leading edge of the cavity to the point of surface turbulent transition as well as to the

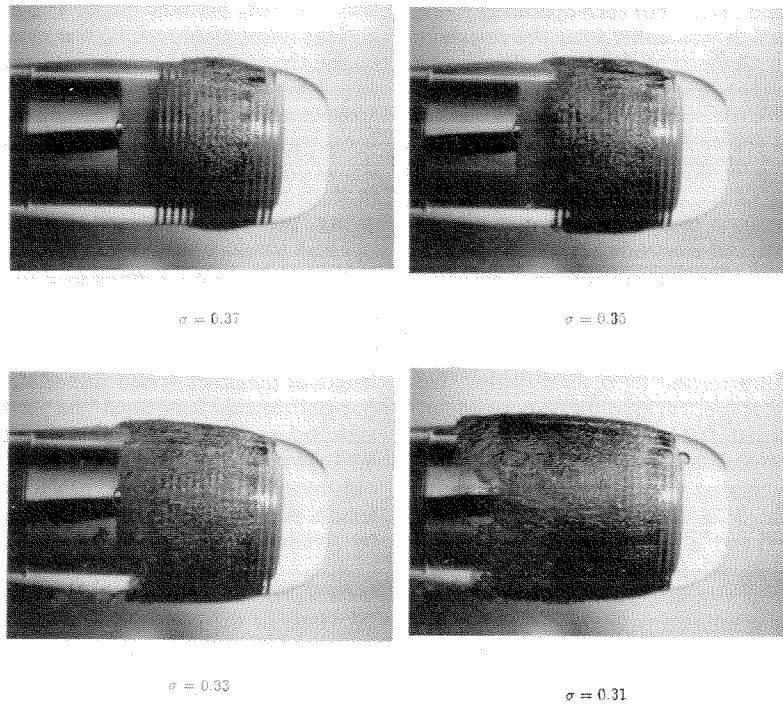


Fig. 8 Examples of attached cavities on the I. T. T. C. body for cavitation numbers $\sigma = 0.37, 0.35, 0.33,$ and 0.31 at a free-stream velocity of $U = 8.7 \text{ m/s}$

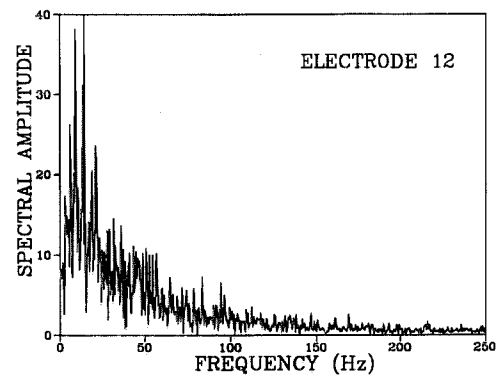
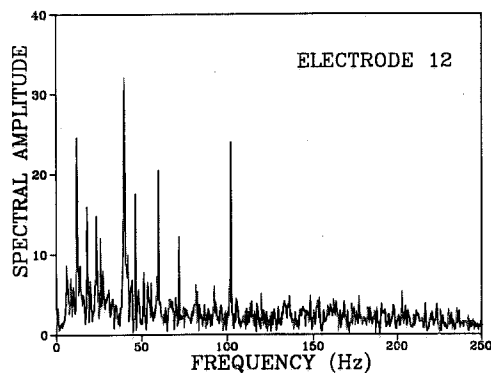
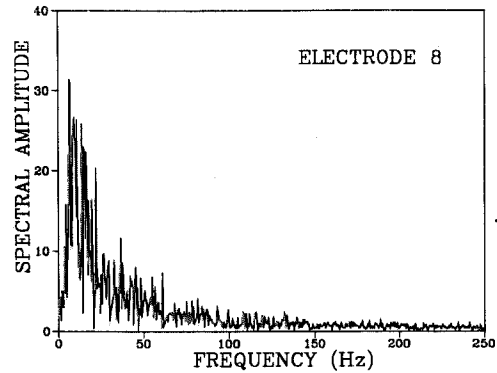
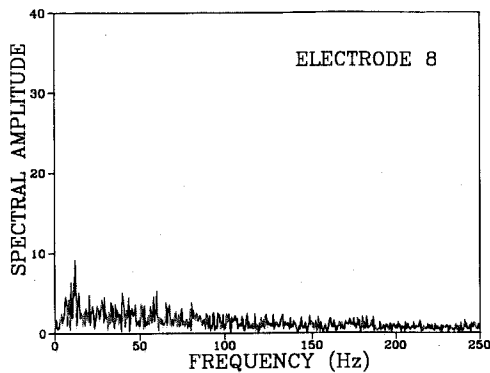


Fig. 9 Electrode signal spectra for cavitation on the I. T. T. C. body with circular electrodes. Cavitation number $\sigma = 0.37$ at freestream velocity $U = 8.75 \text{ m/s}$. The signals were taken from electrode 8 and 12. Vertical scale is arbitrary, and the uncertainty of the spectral coefficients is ± 0.25 .

Fig. 10 Electrode signal spectra for cavitation on the I. T. T. C. body with circular electrodes. Cavitation number $\sigma = 0.31$ at free-stream velocity $U = 8.75 \text{ m/s}$. The signals were taken from electrode 8 and 12. Vertical scale is arbitrary, and the uncertainty of the spectral coefficients is ± 0.25 .

presence of the laminar separation. The first I. T. T. C. body tested was instrumented with sixteen circumferential electrodes, and in order to eliminate any signal which may be due to circumferential oscillations, all the electrode data was taken

for fully developed cavitation which covered the entire circumference.

During the electrical impedance measurements with the I. T. T. C. bodies, attention was focused on the downstream

portion of the fully developed cavity. For each operating point, an electrode was chosen which was either near the region of cavity closure, or completely covered by the cavity. The signals from these electrodes were then Fourier analyzed. The sample spectra in Figs. 9 and 10 are for operating points represented by two of the photographs shown in Fig. 8. Two spectra corresponding to the case of $\sigma = 0.37$ and $U = 8.75$ m/s are shown in Fig. 9. The signals were taken from electrode 8 (as counted from the first electrode upstream), which was completely covered by the cavity, and electrode 12, which was near the cavity reattachment point. The signal from the completely covered electrode exhibits some distinct frequencies, which may be due to cavity surface fluctuations, but these features do not dominate the spectra. Near the cavity closure region, however, the spectra is characterized by several distinct frequencies, with the four largest spectral amplitudes corresponding to frequencies of 12, 40, 60, 102 Hz. These correspond the Strouhal numbers of $St = 0.002, 0.007, 0.010,$ and 0.017 , respectively. The error associated with the Strouhal number measurement is approximately ± 20 percent for the cavities with $\sigma > 0.37$ (thin cavities) and ± 25 percent for the cavities with $\sigma < 0.37$ (thick cavities). (Note that the 60 Hz peak was determined not to be the result of line noise). In general, the frequencies of fluctuations measured near the closure region were repeatable over the range of freestream velocities and cavitation numbers tested.

For the case of $\sigma = 0.31$ presented in Fig. 10, both electrodes 8 and 12 were covered by the cavity. These spectra are dominated by low frequencies and do not exhibit any dominant features. As in the case of the Schiebe body, these low frequency fluctuations are in the range of 0 to 50 Hz. These measurements were from the electrode covered by the fully turbulent region of the cavity, and the principle cause of these signals is the churning of the frothy mixture inside the cavity. The magnitude of the low frequency oscillations increased with decreasing cavitation number and the associated increase in cavity thickness at the location of the electrode. With increasing cavity thickness, the two-phase mixture inside the cavity may begin to churn with a coherent, low-frequency motion. This may not be possible in thin cavities.

The range of frequencies associated with the longitudinal fluctuations of the Schiebe body cavities are quite similar to those measured in the cavity closure region of the I. T. T. C. body. This suggests that similar pulsation mechanisms are present for the two headforms. Furthermore, a I. T. T. C. body with patch electrodes was used to measure the oscillation of the cavity closure region at a specific point on the body surface, and these data were compared to those measurements taken with the circumferential electrodes. The patch electrode spectra were similar to those from the circular electrode data presented above. Similar dominant frequencies were detected near the cavity closure region, although the relative magnitude of the spectral peaks were reduced. This result suggests that the pulsation mechanism operates in a similar way over the entire surface of the cavity.

The cavities observed on the I. T. T. C. body (as well as the Schiebe body) had relatively constant lengths and have been referred to as "stabilized partial cavities" (Knapp et al., 1970). Previous observations of these cavities have revealed the presence of local, periodic fluctuations near the cavity closure region (Knapp, 1955). These oscillations have been attributed to a reentrant jet which cause the cavity to undergo a process of filling and break-off. At the free-stream velocities of this study, the cavities did not undergo large scale filling and breaking, since the re-entrant jet may not be able to penetrate far upstream in the cavity. Instead, premature growth and break-off may occur. Knapp observed that large scale shedding occurred at frequencies on the order of 50 to 130 Hz on a 2 in. diameter, hemisphere shaped axisymmetric bodies, for various velocities and cavitation numbers. As the velocity

was lowered, periodic vapor entrainment became noticeable, and the filling and breaking process was reduced. In the present study, the measured frequencies of cavity oscillation were on the same order as those measured previously, although the freestream velocities were much lower. Small scale filling and breaking along with periodic entrainment of vapor would cause the cavity to oscillate in size, leading to periodic fluctuations in both the lateral boundaries and the closure region of the cavity, such as those observed here.

These results may also be compared to the shedding of cavitation vortices in the wake of a bluff body. Young and Holl (1966) observed that cavitation vortices were shed from a symmetric wedge with Strouhal numbers on the order of 0.26, based on the shedding frequency, freestream velocity, and the length of the downstream side of the wedge. For a thin wedge, one half of this length may be related to the thickness of an attached cavity resulting in a modified Strouhal number of 0.13. These measurements were conducted at an average Reynolds number of 1.7×10^5 based on the characteristic wedge length. A result similar to that of Young and Holl was obtained by Avellan et al., (1988) who measured the vortex shedding of attached cavities on two dimensional hydrofoils. The measured Strouhal number was 0.147 (based on the displacement thickness of the shear layer above the cavity), at a Reynolds number 2×10^6 (based on the cord length). These Strouhal numbers are approximately ten times greater than the values presented in this study, suggesting that the oscillations in the cavity closure region of stable cavities may not be the result of fully developed Kármán vortex shedding.

5 Conclusions

The fluid impedance measurement described in this paper allow determination of both the average size and the dynamic fluctuations of attached cavities. Cavity size may be inferred from the average electrode signal, and with the proper electrode geometry, the total cavity area may be measured. The dynamics of the attached cavity may also be detected through processing of the unsteady component of the electrode signal.

Limited cavitation on the Schiebe body consisted of a series of both steady and intermittent partial cavities. As the cavitation number decreases, the cavities merge to cover the circumference of the headform. These finger cavities fluctuate with distinct frequencies corresponding to Strouhal numbers in the range $St = 0.002$ to 0.02 , and these fluctuations may be caused by cavity oscillations in the circumferential direction. Fully developed cavities produced signals which fluctuate in the frequency range of 0 to 50 Hz, and these oscillations may be the result of intermittent contact of finger cavity boundaries or by churning of a frothy mixture of vapor and liquid inside the cavity.

Cavitation on the I. T. T. C. body started as a single patch on the upper surface of the headform. This grew to cover the entire circumference of the headform as the cavitation number was reduced. The closure region was found to oscillate with distinct frequencies corresponding to Strouhal numbers ranging from $St = 0.002$ to 0.02 . These values are approximately one tenth of the Strouhal numbers associated with Kármán vortex shedding. The cavity in many instances was not evacuated but contained a mixture of vapor and fluid which churned inside the cavity, producing low frequency electrode signals in the frequency range of 0 to 50 Hz. As the cavity became fully developed, the magnitude of the low frequency oscillations increased.

All the cavities of this study had relatively constant lengths and have been referred to as "stabilized partial cavities." The present study has emphasized that these cavities undergo localized fluctuations in the lateral boundaries and the closure region. These fluctuations may be due to the periodic entrainment of cavity vapor and the presence of a small re-entrant

jet which enters the downstream portion of the cavity, causing a process of filling and shedding. In contrast, many cavities exhibit large scale break-off (Knapp, 1955) and (Lush and Skipp, 1986). Cavitation erosion may be related to the shedding of vortices formed over the cavity surface which carry away vapor filaments from the closure region (Avellan et al., 1988). These vapor filaments later collapse in the high pressure region downstream of the cavity causing cavitation erosion. Large scale cavity fluctuations and vapor shedding usually occur at higher Reynolds numbers and were not observed in this study.

Acknowledgments

The authors thank the Office of Naval Research for their support under contract N00014-85-K-0397. The assistance of Yan Kuhn de Chizelle and Sanjay Kumar is gratefully acknowledged, and the authors wish to thank the reviewers for their helpful comments.

References

- Arakeri, V. H. and Acosta, A. J., 1973, "Viscous Effects on the Inception of Cavitation on Axisymmetric Bodies," *ASME JOURNAL OF FLUIDS ENGINEERING*, Vol. 95, pp. 519-527.
- Avellan, F., Dupont, P., and Ryhming, I., 1988, "Generation Mechanisms and Dynamics of Cavitation Vortices Downstream of a Fixed Leading Edge Cavity," *Proc. Seventeenth Symp. on Naval Hydrodynamics*, The Hague, pp. 317-329.
- Blake, W. K., Wolpert, M. J., and Geib, F. E., 1977, "Cavitation Noise and Inception as Influenced by Boundary Layer Development on a Hydrofoil," *J. of Fluid Mechanics*, Vol. 80, pp. 617-640.
- Brennen, C. E., 1970, "Cavity Surface Wave Patterns and General Appearance," *J. of Fluid Mechanics*, Vol. 80, pp. 617-640.
- Ceccio, S. L., 1990, "Observations of the Dynamics and Acoustics of Travelling Bubble Cavitation," Caltech Div. Engineering and Applied Science Rep. No. ENG249.11.
- Ceccio, S. L. and Brennen, C. E., 1991, "Observations of the Dynamics and Acoustics of Travelling Bubble Cavitation," accepted for publication in the *J. of Fluid Mechanics*.
- Emerson, A., and Sinclair, L., 1967, "Propeller Cavitation: Systematic Series Tests on 5- and 6- Bladed Model Propellers," *SNAME Trans.*, Vol. 75, pp. 224-267.
- Gates, E. M., 1977, "The Influence of Freestream Turbulence, Freestream Nuclei Populations, and Drag-Reducing Polymer on Cavitation Inception on Two Axisymmetric Bodies," Caltech Div. Engineering and Applied Science Rep. No. E182-2.
- Gates, E. M., Billet, M. L., Katz, J., Ooi, K. K., Holl, W., and Acosta, A. J., 1979, "Cavitation Inception and Nuclei Distribution- Joint ARL-CIT Experiments," Caltech Div. Engineering and Applied Science Rep. No. E244.1.
- Knapp, R. T., 1955, "Recent Investigations of the Mechanisms of Cavitation and Cavitation Damage," *Trans. ASME*, Vol. 77, pp. 1045-1055.
- Knapp, R. T., Daily, J. W., and Hammit, F. G., 1970, *Cavitation*, McGraw-Hill.
- Lingren, H. and Johnsson, C. A., 1966, "Cavitation Inception on Headforms: I. T. T. C. Comparative Experiments," *Proc. Eleventh Int. Towing Tank Conf.*, Tokyo.
- Lush, P. A. and Skipp, S. R., 1986, "High Speed Cine Observations of Cavitating Flow in a Duct," *Int. J. of Heat and Fluid Flow*, Vol. 7, pp. 283-290.
- Schiebe, F. R., 1972, "Measurement of the Cavitation Susceptibility of Water Using Standard Bodies," U. of Minnesota St. Anthony Falls Hydraulic Lab. Rep. No. 118.
- Weitendorf, E. A., 1989, "25 Years of Research on Propeller Excited Pressure Fluctuations and Cavitation," *Proc. Third Int. ASME Symp. on Cavitation Noise and Erosion in Fluid Systems*, San Francisco, pp. 1-10.
- Young, J. O. and Hall, J. W., 1966, "Effects of Cavitation on Periodic Wakes Behind Symmetric Wedges," *Trans. ASME*, Vol. 88, pp. 163-176.